Performance of the Monitoring Light Source for the CMS Lead Tungstate Crystal Calorimeter

Liyuan Zhang, *Member, IEEE*, David Bailleux, Adolf Bornheim, Kejun Zhu, and Ren-yuan Zhu, *Senior Member, IEEE*

***Abstract*—Light monitoring will play a crucial role in maintaining energy resolution for the CMS lead tungstate crystal calorimeter at LHC. In the last several years, a laser based monitoring light source was designed and constructed at Caltech, and was installed and commissioned at CERN. This paper presents the design of the CMS ECAL monitoring light source and its performance during beam tests. Issues related to the monitoring precision are discussed.**

***Index Terms*—Calorimeter, crystal, laser, lead tungstate, monitoring, radiation hardness, scintillator.**

I. Introduction

THE main physics motivation for building the Compact Muon Solenoid (CMS) experiment at Large Hadron Collider (LHC) is to investigate the mechanism responsible for electroweak symmetry breaking. In the low mass range between 115 and 150 GeV the Higgs discovery potential in the $\gamma\gamma$ decay channel is directly related to the reconstructed mass width, or the energy resolution of the electromagnetic calorimeter (ECAL). The CMS lead tungstate ($PbWO_4$ or PWO) crystal ECAL has a designed energy resolution

$$\frac{\sigma E}{E} = \frac{\mathbf{2.5\%}}{\sqrt{E}} \oplus \mathbf{0.55\%} \oplus \frac{0.2}{E} \tag{1}$$

for the barrel and

$$\frac{\sigma E}{E} = \frac{\mathbf{5.7\%}}{\sqrt{E}} \oplus \mathbf{0.55\%} \oplus \frac{0.25}{E} \tag{2}$$

for the endcaps, where $\oplus$ stands for addition in quadrature and E is in GeV [1]. Test beams at CERN have shown that this energy resolution can be achieved by using mass-produced PWO crystals with avalanche photodiode (APD) readout [2]. A crucial issue, however, is to maintain this energy resolution, especially the constant term, *in situ* at LHC.

II. Lead Tungstate Crystal Radiation Damage

Because of the high energy and high luminosity at the LHC the CMS detector will be operated in a severe radiation environment. The mass produced lead tungstate crystals are radiation hard to high integrated dosage, but suffer from a dose rate dependent radiation damage as shown in induced absorption [3]. Our previous studies concluded that the scintillation mechanism of PWO is not affected by radiation, and the loss of light output is due only to the radiation induced absorption [4]. Fig. 1 shows no variation of the excitation and emission (photoluminescence) spectra, measured by a Hitachi F-4500 fluorescence spectrophotometer for a PWO sample, before and after extensive γ-ray irradiations with dose rate of 400 rad/h. Within the measurement errors the shape of these spectra are identical, indicating that the scintillation mechanism in PWO crystals is not damaged by the γ-ray irradiations.

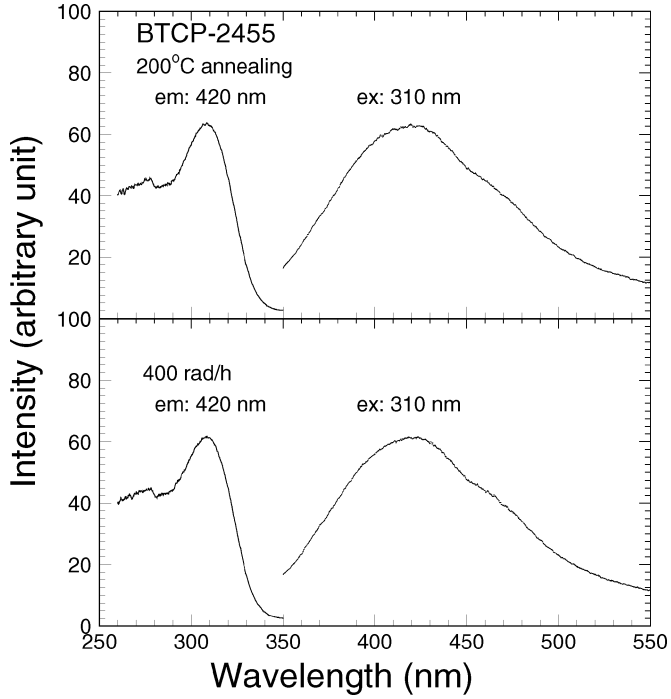

Fig. 1. Excitation and emission (photoluminescence) spectra, measured by a Hitachi F-4500 fluorescence spectrophotometer, for a PWO sample before and after irradiation at 400 rad/h are shown as function of wavelength.

Although there is no damage to the scintillation mechanism, color centers are created during irradiations. It is known that radiation induced color centers may annihilate at room temperature. During irradiations both annihilation and creation processes coexist, so the color center density reaches an equilibrium at a level depending on the dose rate applied. Assuming the annihilation speed of the color center i is proportional to a constant a_i and its creation speed is proportional to a constant

Manuscript received November 15, 2004; revised March 31, 2005. This work was supported in part by the U.S. Department of Energy under Grant DE-FG03-92-ER40701.

The authors are with the California Institute of Technology, Pasadena, CA 91125 USA (e-mail: liyuan@hep.caltech.edu).

Digital Object Identifier 10.1109/TNS.2005.852661

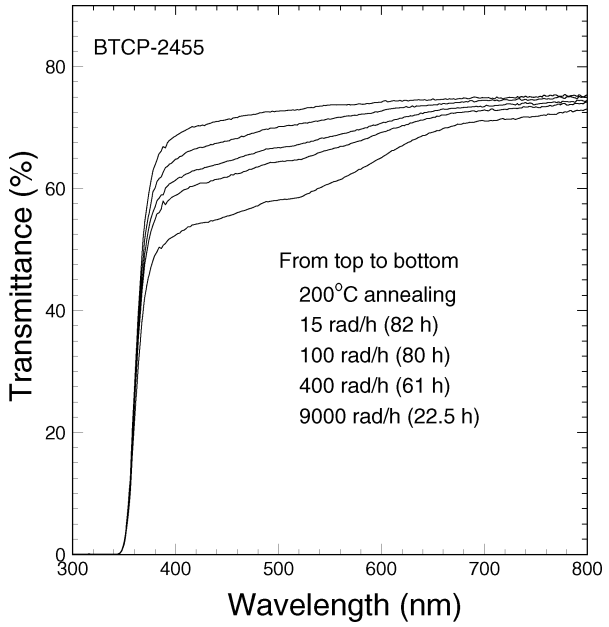

Fig. 2. Longitudinal transmittance spectra, measured by a Hitachi U-3210 UV/visible spectrophotometer, for a PWO sample at equilibrium under γ-ray irradiations of several dose rates are shown as function of wavelength.

b_i and the dose rate (R), the differential variation of color center density when both processes coexist can be written as [4]

$$dD = \sum_{i=1}^{n} \{-a_i D_i + (D_i^{all} - D_i)\, b_i R\} dt \tag{3}$$

where D_i is the density of the color center i in the crystal and the summation goes through all centers. The solution of (3) is

$$D = \sum_{i=1}^{n} \left\{ \frac{b_i R D_i^{all}}{a_i + b_i R} \left[1 - e^{-(a_i + b_i R)t}\right] + D_i^0 e^{-(a_i + b_i R)t} \right\} \tag{4}$$

where D_i^{all} is the total density of the trap related to the center i and D_i^0 is its initial density. The color center density in equilibrium (D_{eq}) depends on the dose rate (R) applied

$$D_{eq} = \sum_{i=1}^{n} \frac{b_i R D_i^{all}}{a_i + b_i R}. \tag{5}$$

Fig. 2 shows longitudinal transmittance spectra, measured by a Hitachi U-3210 UV/visible spectrophotometer for a PWO sample. The curves in the figure, in order from top to bottom, represent the longitudinal transmittance spectra before irradiation and when it reached an equilibrium under a specified dose rate shown in the figure. The longitudinal transmittance data can be used to calculated emission weighted radiation induced absorption coefficient (*EWRIAC*), which is defined as

$$\mathrm{EWRIAC} = \frac{\int \mathrm{Riac}(\lambda) Em(\lambda) d\lambda}{\int Em(\lambda) d\lambda} \tag{6}$$

where $\mathrm{Riac}(\lambda)$ is the radiation induced absorption coefficient or color center density, and $Em(\lambda)$ is the intensity of the scintillation emission. The inverse of the *EWRIAC* can be seen as the degraded light attenuation length. The radiation induced absorption coefficient (Riac), or color center density, were calculated according to an equation

$$\mathrm{Riac} = \frac{1}{\mathrm{LAL}_{\mathrm{equilibrium}}} - \frac{1}{\mathrm{LAL}_{\mathrm{before}}} \tag{7}$$

where the subscripts "equilibrium" and "before" refer to "in equilibrium" and "before irradiation" respectively. The *LAL* is the light attenuation length calculated by using the longitudinal transmittance according to

$$\mathrm{LAL} = \frac{\ell}{\ln\left\{ \frac{[T(1-T_s)^2]}{[\sqrt{4T_s^4 + T^2(1-T_s^2)^2} - 2T_s^2]} \right\}} \tag{8}$$

where T is the transmittance measured along crystal length ℓ and T_s is the theoretical transmittance without internal absorption

$$T_s = (1-R)^2 + R^2(1-R)^2 + \cdots = \frac{(1-R)}{(1+R)} \tag{9}$$

and

$$R = \frac{(n_{\mathrm{crystal}} - n_{\mathrm{air}})^2}{(n_{\mathrm{crystal}} + n_{\mathrm{air}})^2}. \tag{10}$$

Fig. 3 shows a history of *EWRIAC* (solid dots with error bars) for a PWO sample under γ-ray irradiations. Measurements were done step by step at several dose rates: 15, 100, 400, 9,000 and 35 000 rad/h. The *EWRIAC* data confirms dose rate dependent radiation damage in PWO crystals. The numerical value of *EWRIAC* for this PWO sample is less than 1.1 m^{-1}, indicating that its light response uniformity, and thus energy resolution, is not be affected [4]. The radiation induced absorption and its recovery, however, affect crystal's light output. Fig. 4 shows the measured light output normalized to that before irradiations (solid dots with error bars) as a function of time for a PWO sample under γ-ray irradiations. Measurements were done step by step for several dose rates, 15, 100, 500 and 1,000 rad/h, and followed by a recovery process at room temperature. The CMS ECAL monitoring system is designed to correct variation of Crystal's light output caused by color center formation and recovery.

III. Monitoring Light Source Specification

A precise calibration *in situ* is crucial in maintaining the precision offered by a crystal calorimeter. For the CMS PWO calorimeter, a light monitoring system is designed to measure variations of crystal's optical transmission and use that to project variations of the light output [5]. The monitoring light pulses produced by a laser system are distributed via an optical fiber system organized into three levels: a fiberoptic switch which sends laser pulses to one of 80 calorimeter elements (72 1/2 super module in the barrel and 8 groups of super crystals in two endcaps), and a two stage distribution system mounted on each calorimeter element which delivers monitoring pulses to each individual crystal [1]. The monitoring system is required to measure relative variations of crystal transmission with 0.1% precision by using reference photodiodes as normalization.

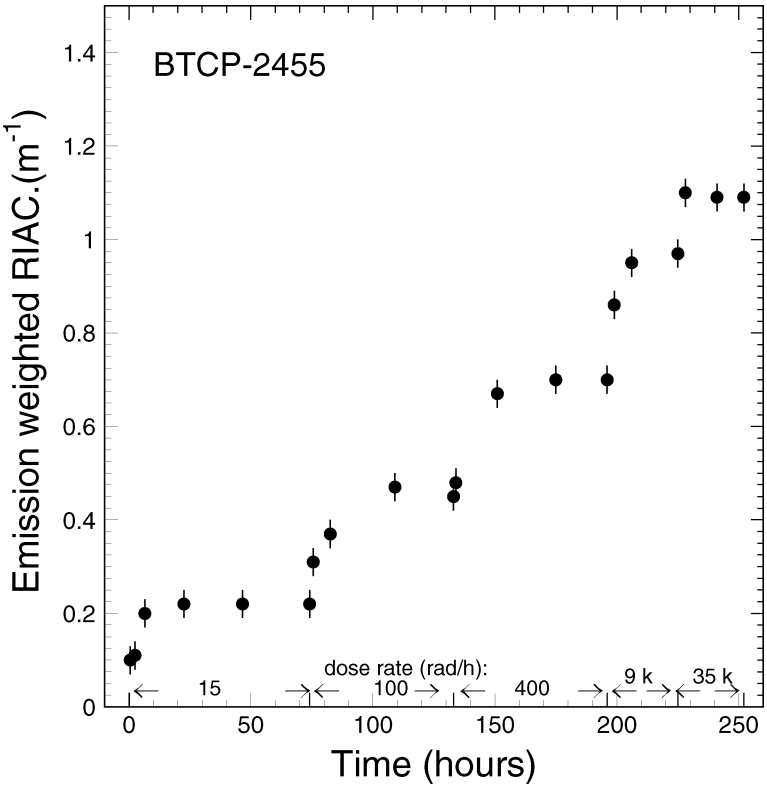

Fig. 3. Emission weighted radiation induced absorption coefficient (*EWRIAC*) are shown as function of time for a PWO sample under γ-ray irradiations of several dose rates.

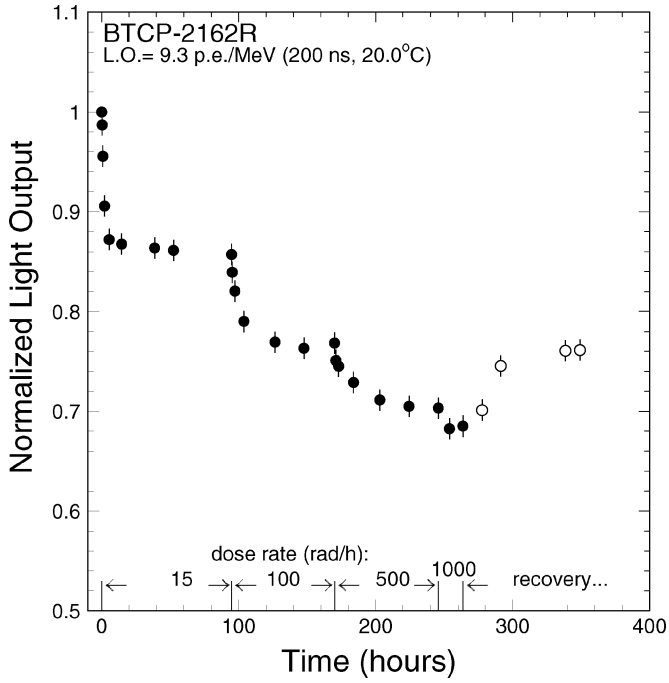

Fig. 4. Damage and recovery history of light output are shown as function of time for a PWO sample under γ-ray irradiations of several dose rates.

This precision was achieved in beam tests lasted for several weeks [6]. Combined with crystal response to physics events, such as electron pairs from the Z^0 decays and single electrons from the W decays, calibration precision at a level of 0.4% is expected to be achieved for the CMS PWO crystal ECAL *in situ* at LHC, and thus maintaining the constant term of the ECAL energy resolution as shown in (1) and (2).

The specification for the laser based monitoring light source is listed below [8].

- Two Wavelengths: One close to the emission peak which provides the best monitoring linearity for the PWO crystals, and the other provides cross checks.
- Spectral Contamination: $< 10^{-3}$.
- Pulse Width: Full width at half maximum (FWHM) $<$ 40 ns to match the ECAL readout.
- Pulse Jitters: < 3 ns for trigger synchronization to the LHC beam.
- Pulse Rate: ~ 80 Hz, which is the rate at which the "spy mode" ECAL DAQ used for monitoring events can operate.
- Pulse Energy: 1 mJ/pulse at monitoring wavelength, corresponding to 1.3 TeV in full dynamic range, and a linear attenuator at 1% step down to 13 GeV.
- Pulse Intensity Instability: $< 10\%$ to guarantee monitoring precision of 0.1% by using a Si photodiode normalization.

To continuously track variations of crystal light output caused by radiation damage and its recovery the monitoring system is required to be operational 100% of the time during the data taking [7]. To provide continuous monitoring, about 1% of the 3.17 μs beam gap in every 88.924 μs LHC beam cycle [9] will be used to inject monitoring light pulses into crystals. The time needed to scan the entire ECAL is expected to be about 30 min [8].

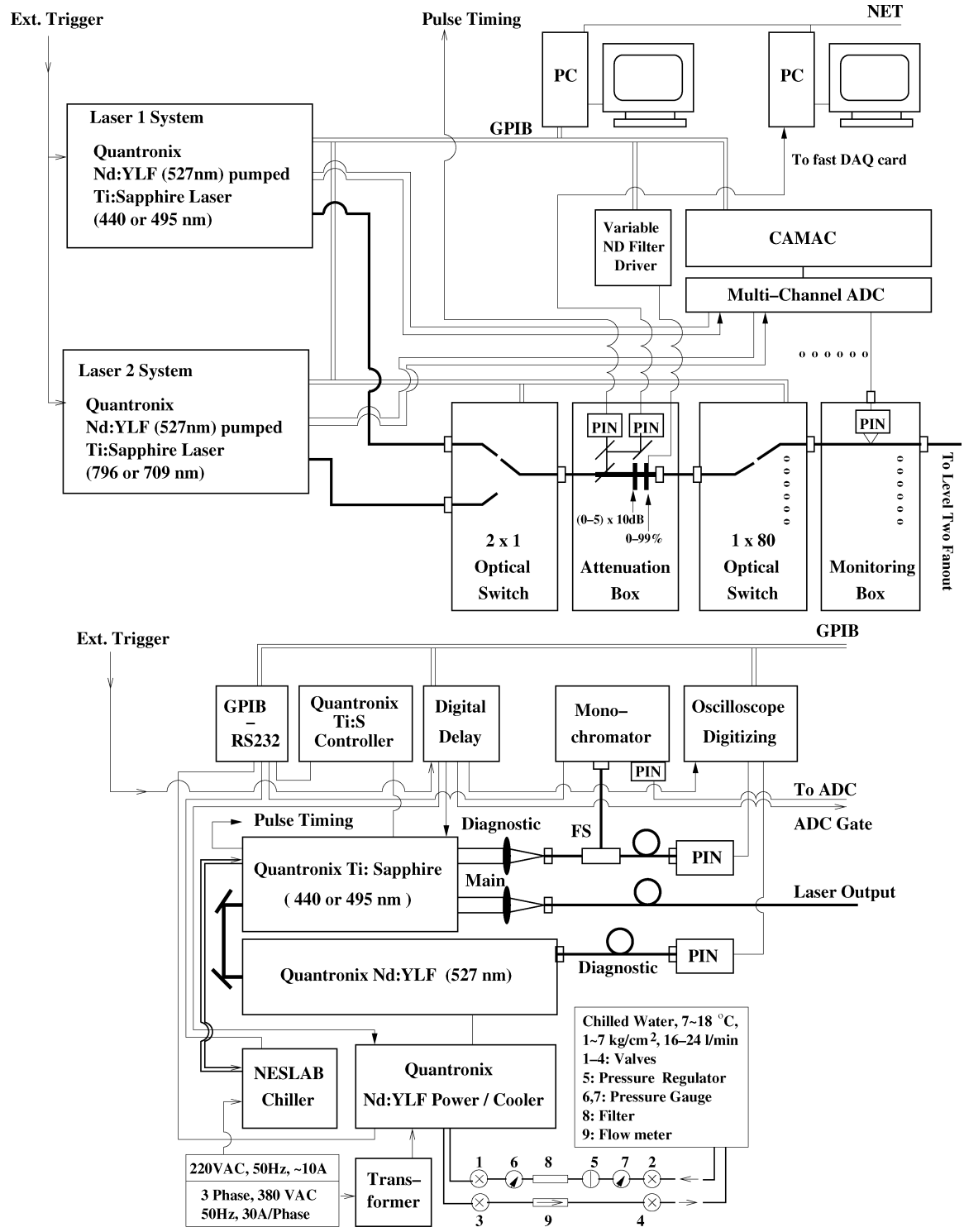

Fig. 5. (Top) Schematic showing the design of the laser based monitoring light source and high level distribution system, and (bottom) the details of one laser system.

IV. Monitoring Light Source Design

The CMS ECAL monitoring light source consists of three laser systems, each with their own diagnostics, two fiberoptic switches, internal monitors and corresponding PC based controllers. Fig. 5 is a schematic showing the design of the monitoring light source and high level distribution system (Top) and the details of a laser system (Bottom). As shown in this figure each laser system consists of an Nd:YLF pump laser (Fig. 6 back), its power supply and cooler unit and corresponding transformer, a Ti:Sapphire laser (Fig. 6 front) and its controller, and a NESLAB cooler for an LBO crystal in the Ti:S laser. Each pair of the YLF and Ti:S lasers and their corresponding optics are mounted on an optical table.

Fig. 6. (Back) Photo of the Quantronix laser system showing the Nd:YLF pump laser and (front) the tunable Ti:S laser.

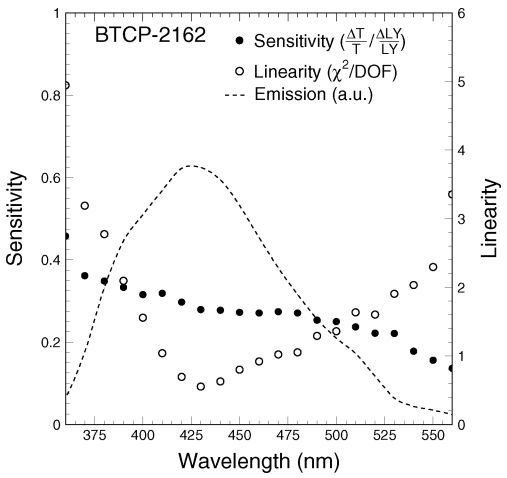

Fig. 7. Monitoring sensitivity, linearity and emission spectrum are shown for a PWO sample.

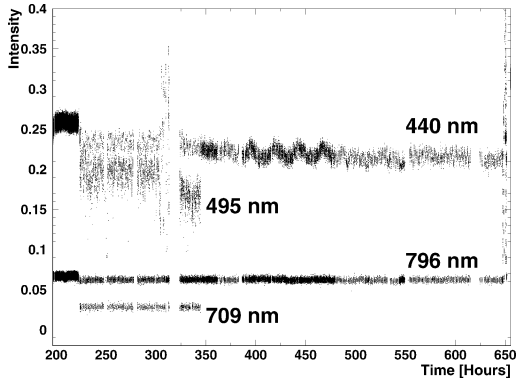

Fig. 8. Laser pulse intensity at 440, 495, 796 and 709 nm is shown as function of time during a 19 day period in a beam test at CERN. Vertical spreads in the middle left (320 h) and right (650 h) are laser pulse energy scan runs for electronics tests.

The choice of monitoring wavelength directly affects the monitoring sensitivity and linearity [5]. Fig. 7 shows the monitoring sensitivity (the slope of a linear fit to $\Delta T/T$ versus $\Delta LY/LY$, where T and LY refer to the transmission and the light yield respectively) and the linearity (χ^2/DOF of the fit) as a function of the monitoring wavelength for a PWO sample. Also shown in the figure is the PMT quantum efficiency weighted radio luminescence. The higher monitoring sensitivity at shorter wavelength is understood because of the lower initial transmittance as compared to that at the longer wavelength. The best linearity around the peak of the radio luminescence is understood by two radiation-induced color centers peaked at the two sides of the luminescence peak with different damage and recovery speed [5]. Based upon this result, 440 nm (blue) was chosen as the monitoring wavelength. In addition, 796 nm (infrared) is used to monitor independently the gain variations of the readout electronics chain from the APD to the ADC.

All three pump lasers are model 527DQ-S Q-switched Nd:YLF lasers, which are commercial product by Quantronix Inc. [10]. It provides frequency doubled laser pulses at 527 nm with a pulse intensity up to 20 mJ at a repetition rate up to 1 kHz. All three Ti:S lasers are custom made Proteus UV(SHG) lasers from Quantronix, which provide the laser pulse intensity up to 1 mJ at repetition rate up to 100 Hz [8]. This laser pulse intensity corresponds to about 1.3 TeV electromagnetic energy deposition in PWO crystals. Two wavelengths are available for each Ti:S laser, which is tunable by choosing the appropriate built-in interference filter. Each set of lasers has a main output and a diagnostic output. The diagnostic output is further split to two fibers by using a fiber splitter. One output goes to a monochromator for wavelength spectrum monitoring, while the other goes to a digital scope which samples pulse energy, width and timing at a rate about 1 Hz. The histograms and history of laser pulse energy, FWHM, timing and wavelength spectra obtained by the digital scope and the monochromator are stored in computer.

As shown in Fig. 5, the monitoring light source in operation consists of two laser systems, so that a total of 4 wavelengths, 440 nm (blue), 495 nm (green), 709 nm (red) and 796 nm (infrared), are available by using a 2×1 optical switch [11]. The output of this switch goes to a monitoring box, which measures laser pulse energy and FWHM by using an Acqiris DP210 digitizer card sampling each laser pulse at 2 GS/s and provides a logarithmic attenuator and a computer controlled linear polarizer, which attenuates the pulse energy at 1% step down to 1% (13 GeV), for the main laser output. The output of the monitoring box is distributed via a 1×80 fiberoptic switch to 80 calorimeter elements through 150 m long quartz fibers. The histograms and history of pulse energy and FWHM are also stored in the computer. The third laser system is a spare laser, which also runs at 440 nm (blue) and 495 nm (green) to guarantee

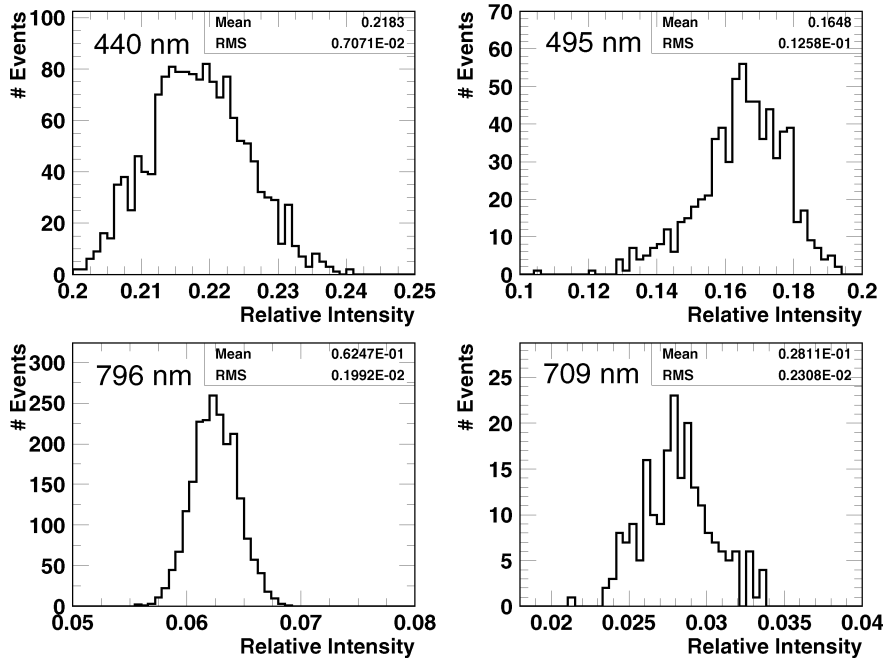

Fig. 9. Distribution of laser pulse energy obtained in 25 h for four wavelengths.

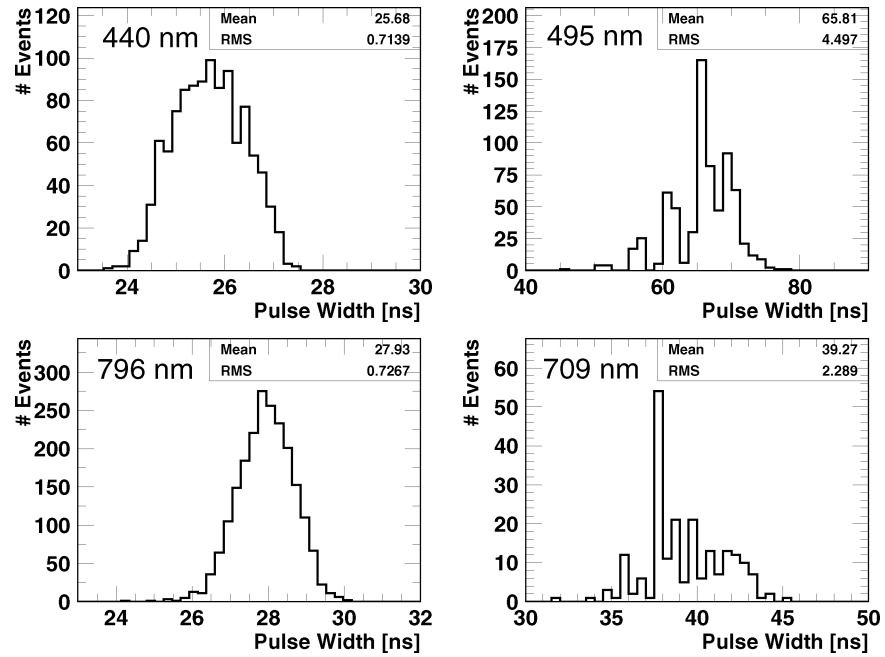

Fig. 10. Distribution of laser pulse width obtained in 25 h for four wavelengths.

100% availability of the main monitoring wavelength at 440 nm even during laser maintenance [7]. This spare laser system has its own control, so can be used independently.

V. Monitoring Light Source Performance

The first blue/green laser system and its corresponding diagnostics were installed and commissioned at CERN in August, 2001 [12], and has been used in beam tests since then. In August 2003, the IR/red and the second blue/green laser system was installed and commissioned at CERN [13]. All three laser systems are housed in a laser barracks with air conditions and safety features. Fig. 8 shows a typical history of the laser pulse intensity in a 19 day run during a beam test at CERN. All four wavelengths are used. Pulse intensity scans by using the linear polarizer were carried out to test the linearity of the readout electronics.

The short term r.m.s. spread of the laser system in 30 min is typically at a level of 1% to 2%. Figs. 9 and 10 show laser pulse energy and FWHM distributions respectively obtained for four wavelengths in 25 h runs, indicating an r.m.s. spread of the pulse energy and FWHM width are at the 3% level for the blue and IR, and about 7% for the red and green. This difference of r.m.s spread for different wavelengths is well understood. Since the

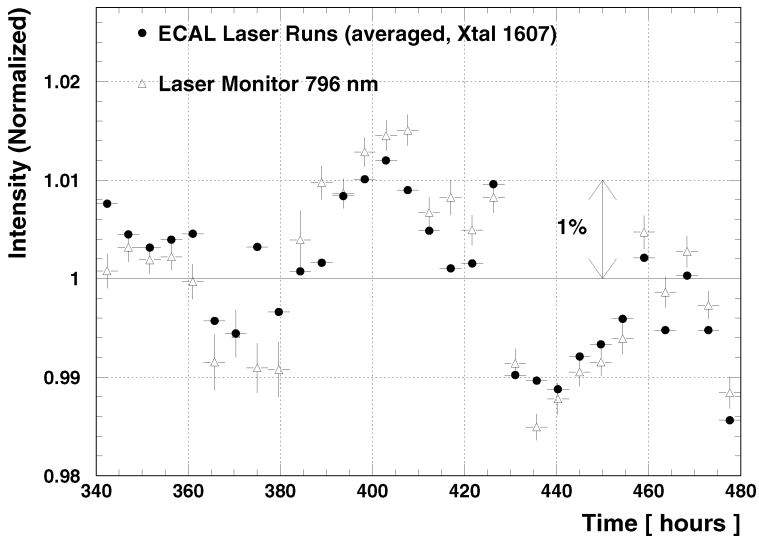

Fig. 11. Comparison of laser pulse intensities measured in 6 days by the ECAL APD readout and the laser internal monitor readout.

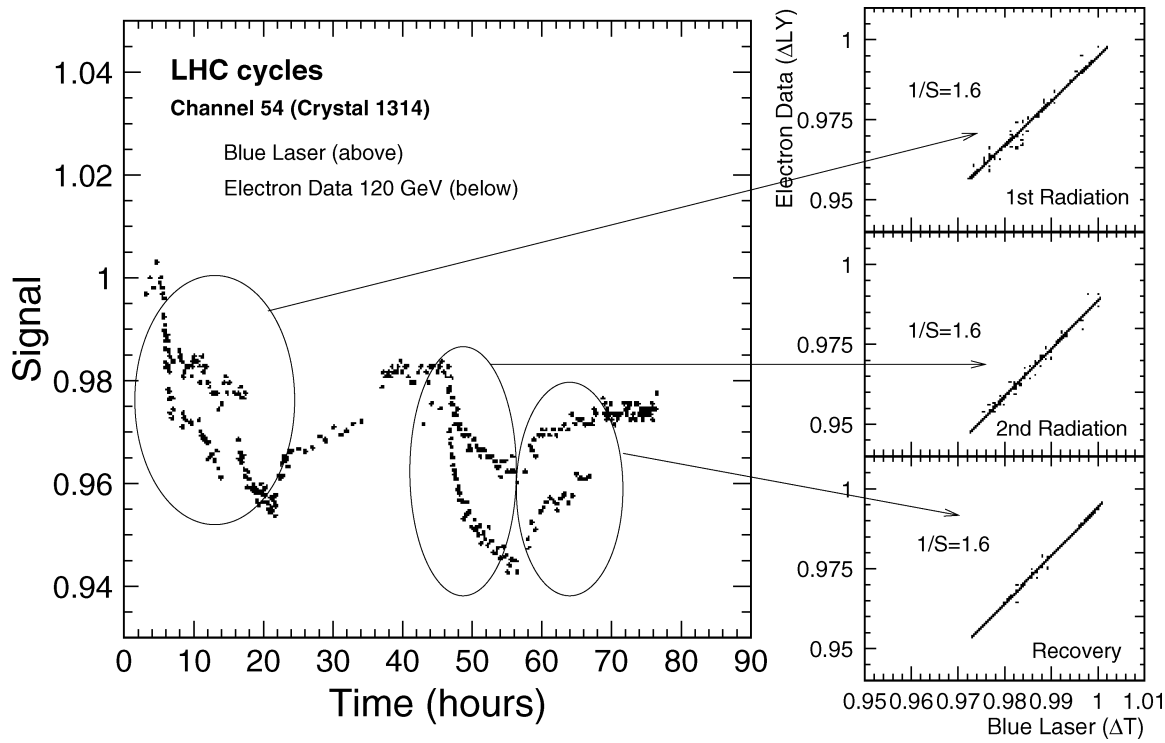

Fig. 12. (Above) 120 GeV electron and (below) 440 nm laser data are shown as function of time during an irradiation beam test. Three expansions at right show the same linearity between electron and the monitoring signals.

Ti:S emission spectrum is peaked at 800 nm with a FWHM of ~ 180 nm, its intensity, and thus the r.m.s. spread, at these four wavelengths degrades in an order of 796 nm, 440 nm (frequency doubled), 709 nm and 495 nm (frequency doubled).

Fig. 11 is a comparison of laser pulse intensity measured by the ECAL APD readout and the laser internal monitors for laser pulses at 796 nm, showing good consistency. The data in this plot are not corrected by the reference diodes. The time dependent variations observed in 6 days are correlated to the temperature variations in the laser barracks. It is known that the Ti:S laser pulse energy and FWHM have a temperature coefficient of $-4\%/$ °C and 1.3 ns/°C respectively [14]. Following this observation and some degradation of laser optics observed during beam tests, a rigorous environmental control is planned to be implemented by using portable clean room facilities with temperature stabilization [14].

The laser based monitoring system was used to follow variations of PWO crystal transmission in beam tests at CERN. Fig. 12 shows 120 GeV electron and 440 nm laser data collected during a beam test when PWO samples were bombarded with electrons to simulate the LHC environment. The damage and recovery processes are clearly seen in the figure. The slopes of variations of light output versus transmission observed in these processes are consistent.

VI. Summary

In the last several years, a laser based monitoring light source was designed and constructed at Caltech, and was installed and commissioned at CERN. The performance of this system exceeds the original specification. While detailed study is under way to understand ultimate performance of this monitoring system and its systematic effects, initial application in beam tests at CERN indicates that this laser based monitoring system will play a crucial role in maintaining the precision of the CMS PWO crystal calorimeter *in situ* at LHC.

Acknowledgment

The authors would like to thank the entire CMS ECAL collaboration for their effort, especially Dr. J. Bourotte, Dr. M. Dejardin, Dr. M. Haguenauer, Dr. J. Rander, and Dr. P. Verrecchia for many discussions.

References

[1] "The Electromagnetic Calorimeter Technical Design Report," CMS Collaboration, CERN/LHCC 97-33, 1997.

[2] E. Auffray *et al.*, "Beam tests of lead tungstate crystal matrices and a silicon strip preshower detector for the CMS electromagnetic calorimeter," *Nucl. Instrum. Meth. A*, vol. 412, pp. 223–237, 1998.

[3] R. H. Mao, L. Y. Zhang, and R. Y. Zhu, "Quality of mass produced lead tungstate crystals," *IEEE Trans. Nucl. Sci.*, vol. 51, no. 4, pp. 1777–1783, Aug. 2004.

[4] R. Y. Zhu, "Radiation damage in scintillating crystals," *Nucl. Instrum. Meth. A*, vol. 413, pp. 297–311, 1998.

[5] X. D. Qu, L. Y. Zhang, and R. Y. Zhu, "Radiation induced color centers and light monitoring for lead tungstate crystals," *IEEE Trans. Nucl. Sci.*, vol. 47, no. 6, pp. 1741–1747, Dec. 2000.

[6] M. Dejardin *et al.*, "Stability studies of the prototype monitoring system for CMS-ECAL," in *Proc. 9th Int. Conf. Calorimetry in Particle Physics*, vol. XXI, Franscati Physics Series, B. Aubert *et al.*, Eds., 2000, pp. 695–700.

[7] L. Y. Zhang, K. J. Zhu, R. Y. Zhu, and D. T. Liu, "Monitoring light source for CMS lead tungstate crystal calorimeter at LHC," *IEEE Trans. Nucl. Sci.*, vol. 48, no. 3, pp. 372–378, Jun. 2001.

[8] L. Y. Zhang, R.-Y. Zhu, and D. Liu, "Monitoring Lasers for PWO ECAL," CMS IN 1999/014.

[9] "The LHC Conceptual Design Report," The LHC Study Group, CERN/AC/95-05 46, 1995.

[10] [Online]. Available: http://www.quantronixlasers.com

[11] L. Y. Zhang and R. Y. Zhu, "Evaluation of a DiCon GP-700 1×2 Optical Switch," CMS IN 1998/031.

[12] L. Y. Zhang, K. J. Zhu, R. Y. Zhu, and D. Liu, "Installation of ECAL Monitoring Light Source," CMS IN 2001/008.

[13] D. Bailleux, A. Bornheim, L. Y. Zhang, K. J. Zhu, R.-Y. Zhu, and D. Liu, "ECAL Monitoring Light Source at H4," CMS IN 2003/045.

[14] R. Y. Zhu. Requirements on ECAL Monitoring Laser Installation at USC55. [Online]. Available: http://www.hep.caltech.edu/zhu/ryz_041 028_usc55.pdf